Received: 1 February 2022 | Revised: 24 April 2022 | Accepted: 9 May 2022

DOI: 10.1002/ntls.202103302

Natural Sciences

RESEARCH ARTICLE

Capture the missing: formation of $(PbBi_3)^{-}$ and $\{[AuPb_5Bi_3]_2\}^{4-}$ via atom exchange or reorganization of the *pseudo*-tetrahedral Zintl anion $(Pb_2Bi_2)^{2-}$

Fuxing Pan | Lukas Guggolz | Stefanie Dehnen

Fachbereich Chemie and Wissenschaftliches Zentrum für Materialwissenschaften, Philipps-Universität Marburg, Marburg, Germany

Correspondence
Stefanie Dehnen, Fachbereich Chemie and Wissenschaftliches Zentrum für Materialwissenschaften, Philipps-Universität Marburg, Hans-Meerwein-Straße 4, 35043 Marburg, Germany.
Email: dehnen@chemie.uni-marburg.de

Abstract

(*Pseudo*-)tetrahedral p-block atom units have been attracting the interest of many scientists, mainly regarding their use as elegant starting materials for compounds with larger molecular or extended architectures. The isoelectronic four-atomic species that were addressed so far span the range from neutral P_4, As_4, and AsP_3, via the homoatomic $Si_4{}^{4-}$ anion and its heavier congeners, to heteroatomic Zintl anions $(TrPn_3)^{2-}$ or $(Tt_2Pn_2)^{2-}$ (Tr = Ga, In, Tl; Tt = Si, Ge, Sn, Pb; Pn = P, As, Sb, Bi). Hence, $(Pb_2Bi_2)^{2-}$ in the salt $[K(crypt\text{-}222)]_2(Pb_2Bi_2)\cdot en$ (en = ethane-1,2-diamine) is isoelectronic and isostructural to white phosphorus, but it exhibits significantly different properties owing to its charge and the different nature of the involved atoms, which affects its stability and reactivity. The recently reported compound $[K(crypt\text{-}222)]_3[Au\{\eta^2\text{-}(Pb_2Bi_2)\}_2]$ (**A**), isolated from reactions of the binary anion with $[AuMePPh_3]$ in en, possesses two intact *pseudo*-tetrahedral $(Pb_2Bi_2)^{2-}$ moieties. In this work, however, the same reaction of $[AuMePPh_3]$ with $[K(crypt\text{-}222)]_2(Pb_2Bi_2)\cdot en$ in pyridine instead of en, and subsequent layering with tetrahydrofuran or toluene, yielded two compounds comprising Zintl anions that have not yet been reported to occur in condensed phase. One of them is the $(PbBi_3)^{-}$ anion, which crystallizes in the triple salt $[K(crypt\text{-}222)]_4[(PbBi_3)(Pb_2Bi_2)(AuMe_2)]\cdot 6py$ (**1**). The second is the Pb/Bi moiety in the cluster anion $\{[AuPb_5Bi_3]_2\}^{4-}$, which was obtained in the compound $[K(crypt\text{-}222)]_4\{[AuPb_5Bi_3]_2\}\cdot 2py$ (**2**). Density functional theory calculations confirm that the $(PbBi_3)^{-}$ monoanion results from an atom exchange reaction whereas $\{[AuPb_5Bi_3]_2\}^{4-}$ was formed upon more significant reorganization of the reactant $(Pb_2Bi_2)^{2-}$ in the presence of Au(I) ions. The trimetallic cluster is the yet missing, heaviest homolog of a series of isostructural species. The new compounds were accessed by a careful selection of the solvent mixtures used for crystallization, which demonstrates the importance of a thorough control of the reaction space.

Key Points:

1. Reactions of (*pseudo*-)tetrahedral anions of p-block (semi-)metals with transition metal compounds were proven to be a very versatile access of larger multi-metallic clusters; we report on the formation and isolation of two predicted, yet so far elusive, species of both types of heterometallic molecules, $(PbBi_3)^-$ and $[(Au_2Pb_5Bi_3)]^{4-}$.
2. By means of computational studies applying high-level density functional theory (DFT) methods, we were able to rationalize the formation of the uncommon anion $(PbBi_3)^-$, which is the first monoanionic (*pseudo*-)tetrahedral molecule. This study confirms both the need and usefulness of DFT calculations in cluster chemistry.
3. Bi- or trimetallic cluster compounds may serve as starting materials for new inter-metallic phases or act as reactive species in solution or in the gas phase for bond activation themselves. Hence, the understanding of their formation and access on the one hand, and the expansion of the elemental combinations contribute to reach such goals for materials science.

KEYWORDS
atom exchange, DFT calculations, reorganization, tetrahedron, Zintl anions

INTRODUCTION

White phosphorus, P_4, and tetra-*tert*-butyltetrahedrane, $(^tBuC)_4$, represent the most prominent tetrahedral molecules, and they have given rise to a tremendous amount of applications in phosphorus chemistry and organic chemistry, respectively.[1] Stepwise "carbon copying" of the C atoms on the tetrahedral vertexes by P atoms resulted in a series of tetrahedral derivatives, such as neutral $(^tBuC)_3P$, $(^tBuC)_2P_2$, and $(HC)P_3$.[2–5] Isoelectronic replacement of one vertex of P_4 by another pnictogen atom or by chalcogenide cations Ch^+ (Ch = S, Se, Te) has led to the isolation of AsP_3 or the corresponding $(ChP_3)^+$ cations, respectively.[6–8] (*Pseudo*-)tetrahedral Zintl-type anions derived from partial or full isoelectronic replacement of vertexes of P_4 by group 13–15 element (semi-)metal atoms paved way to a series of main group (*pseudo*-)tetrahedral anions with overall charges of −8, −5, −4, −3, or −2, which were used as starting materials for the formation of a multitude of binary or ternary (semi-)metal complexes and clusters.[9–12] Among them, the solution chemistry of Tt_4^{4-} (Tt = Si, Ge, Sn, and Pb), $(Tt_2Pn_2)^{2-}$ (Tt/Pn = Ge/P, Ge/As, Sn/Sb, Sn/Bi, Pb/Sb, and Pb/Bi), and $(TrBi_3)^{2-}$ (Tr = Ga, In, and Tl) in liquid ammonia, ethane-1,2-diamine (en), or pyridine (py) has attracted particular attention.[1]

Upon introducing d-block metal atoms, Tt_4^{4-} anions usually maintain their overall intact tetrahedral form in the resulting complexes, such as in $[(MesCu)_2(\eta^3{:}\eta^3\text{-}Tt_4)]^{4-}$ (Tt = Si, Ge), $[(EtZn)_2(\eta^3{:}\eta^3\text{-}Ge_4)]^{2-}$, and $[(\eta^2\text{-}Sn_4)Zn(\eta^3\text{-}Sn_4)]^{6-}$.[13–16] This concept can also be extended to p-block element atoms linking the tetrahedral units, which is exemplified by $[In(\eta^3\text{-}Pb_4)_2]^{5-}$ in the A_5InPb_8 (A = K, Rb) alloy.[17]

It was shown that $(Ge_2Pn_2)^{2-}$ anions (Pn = P, As) undergo atom exchange reactions in solution according to Equation (1), thereby forming the new species $(Ge_3Pn)^{3-}$ and $(GePn_3)^-$ in situ in relatively high yield.[18,19] The observation of the species on the most right-hand side of this equilibrium as a precursor to the formation of larger heteroatomic clusters has not been made so far starting from binary anions, which is why they are given here in square brackets.

$$2(Tt_2Pn_2)^{2-} \rightleftharpoons (Tt_3Pn)^{3-} + (TtPn_3)^{-}[\rightleftharpoons (Tt_4)^{4-} + Pn_4]^{\ddagger} \quad (1)$$

The coexistence of $(Ge_xPn_{4-x})^{x-}$ ($x = 1 - 4$) in solution enhances the flexibility of coordination chemistry with such anions, as they provide a range of different charges and donor atom compositions for d-block metal atoms or ions. This can also afford larger clusters, such as $[Cd_3(\eta^2{:}\eta^3\text{-}Ge_3P)_3]^{3-}$ and $[Au_6(\eta^2{:}\eta^2{:}\eta^2\text{-}Ge_3As)(\eta^2{:}\eta^2{:}\eta^2\text{-}Ge_2As_2)_3]^{3-}$.[19,20]

Density functional theory (DFT) calculations confirmed the exoenergetic character of the exchange reactions (E_{exc}) for $(Ge_2Pn_2)^{2-}$ (−111 kJ mol^{-1} for Pn = P, −110 kJ mol^{-1} for Pn = As).[20,21] In contrast, the heavier analogs of $(Ge_2Pn_2)^{2-}$, such as $(Tt_2Pn_2)^{2-}$ (Tt = Sn/Pb, Pn = Sb/Bi) and $(TrBi_3)^{2-}$ (Tr = Ga, In, Tl), tend to undergo fragmentation and reorganization upon interaction with Lewis-acidic d-/f-block compounds. Consequently, a series of intermetalloid or heterometallic clusters were reported, such as $[U@Pb_7Bi_7]^{3-}$, $[Th@Bi_{12}]^{4-}$, $[Bi@Ga_8(Bi_2)_6]^{q-}$ (q = 3, 5), and $[(Bi_6)Zn_3(TlBi_5)]^{4-}$.[22–25] On the other hand, reactions with softer Lewis acids like the Au(I) cation, $(Tt_2Pn_2)^{2-}$ anions can also stay intact in the resulting complexes $[Au\{\eta^2\text{-}(Tt_2Pn_2)\}_2]^{3-}$ (Tt/Pn = Sn/Sb, Sn/Bi, and Pb/Bi).[1,26,27]

To understand the limits of such decisions pro- or contra-deconstruction of the tetrahedral units, it is essential to further explore these heavy atom anions in the context of atom exchange, fragmentation, and reorganization reactions. According to recent reports, the (relative) stabilities of binary *pseudo*-tetrahedral anions are related to the ratio of the corresponding atomic radii—the exchange reactions become more favorable for smaller differences in the covalent radii of the involved atoms.[20,21] Another highly important parameter is the chosen solvent, as all reorganization steps will undoubtedly involve interactions—if not reactions—with the solvent. To gain more insight into this topic in general and into possible ways to influence the reaction processes, we selected $(Pb_2Bi_2)^{2-}$, with a smaller and $(Pb_2Sb_2)^{2-}$, with a larger difference of the atomic radii, for a reference study.

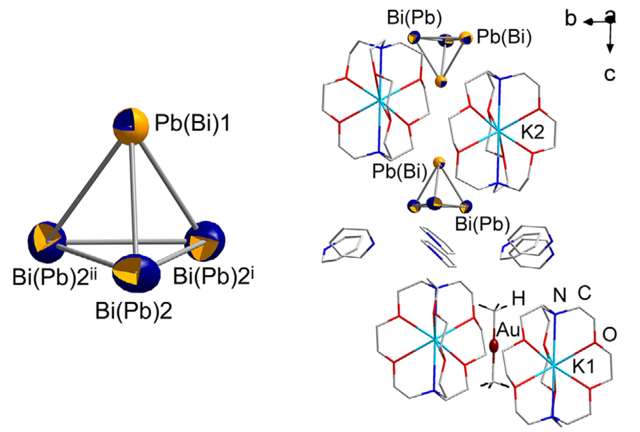

FIGURE 1 Left: A molecular structure of the unprecedented $(PbBi_3)^-$ anion in **1**, with thermal ellipsoids drawn at 50% probability. As Pb and Bi atoms cannot be distinguished from X-ray diffraction experiments, the corresponding atoms are drawn as two-colored atoms (orange–blue), with the assigned atom type being indicated by the dominant color (see text). Selected distances [Å] and angles [°]: Pb(Bi)–Bi(Pb) 3.0293(13), and Bi(Pb)–Bi(Pb) 3.0159(16); Pb/Bi–Bi/Pb–Bi/Pb 59.71(4), 60.00, 60.144(18). Symmetry codes: i = $y-x$, $-x$, z; ii = $-y$, $x-y$, z. Right: asymmetric unit of **1** comprising one $(PbBi_3)^-$ anion, one $(Pb_2Bi_2)^{2-}$ anion, one $[AuMe_2]^-$ anion, four $[K(crypt\text{-}222)]^+$ cations, and six pyridine molecules. Organic groups are given in wire mode for clarity. For more details, see Figures S1, S2, S5, and Tables S1, S2, S5

RESULTS AND DISCUSSION

In addition to the reported $[Au\{\eta^2\text{-}(Pb_2Bi_2)\}_2]^{3-}$ anion in $[K(crypt\text{-}222)]_3[Au\{\eta^2\text{-}(Pb_2Bi_2)\}_2]$ (**A**),[1] which was isolated upon reaction of $(Pb_2Bi_2)^{2-}$ and $[AuMePPh_3]$ in en/tol (tol = toluene) solution, we introduced the same reactants into py/THF (THF = tetrahydrofuran) or py/tol respectively. As a result, we were able to isolate two new anions, $(PbBi_3)^-$ and $\{[AuPb_5Bi_3]_2\}^{4-}$, which crystallized as $[K(crypt\text{-}222)]_4[(PbBi_3)(Pb_2Bi_2)(AuMe_2)]\cdot 6py$ (**1**) and $[K(crypt\text{-}222)]_4\{[AuPb_5Bi_3]_2\}\cdot 2py$ (**2**). Scheme 1 illustrates the formation of the compounds that exhibit an edge-on coordination of two $(Pb_2Bi_2)^{2-}$ anions to a central Au^+ cation while maintaining the intact *pseudo*-tetrahedral geometry in **A**, an atom-exchange reaction in **1**, and a fragmentation and reorganization reaction prior to coordination of an Au(I) atom in **2**.

The importance of the chosen solvent environment for the fragmentation/reorganization process became evident upon changing the solvent from en to pyridine, as this seemed to stabilize the product of the process indicated in Equation (1). Compound **1** crystallizes as reddish-black plates in the trigonal crystal system, space group type $R\bar{3}$ (approx. 60% yield). The salt comprises three types of anions: $[AuMe_2]^-$ and two $(Pb_xBi_{4-x})^{x-}$ *pseudo*-tetrahedral units (see Figure 1). The $[AuMe_2]^-$ complex was previously reported and additionally suggested as one of the side products on the way toward the formation of $\{[AuSn_5Sb_3]_2\}^{4-}$.[27,28] Although the Pb and Bi atoms are not distinguishable by common X-ray diffraction experiments (which also allows for the trigonal symmetry with the threefold axis running through the *pseudo*-tetrahedral anions), we can still assign the atom positions based on the following considerations and experimental evidence: the overall −4 charge of the three anions, which is derived from the presence of four $[K(crypt\text{-}222)]^+$ cations, leave three negative charges for the two *pseudo*-tetrahedral units in the sum. According to the Zintl–Klemm–Busmann *pseudo*-element concept,[29,30] the formal replacement of one Pb^- by one Bi^0 atom will reduce the negative charge by 1. As the presence of a proton for alternative charge compensation was excluded by the use of aprotic solvents and also by NMR studies, there are thus two possible compositions for the two units: (a) either $(PbBi_3)^-$ and $(Pb_2Bi_2)^{2-}$, (b) or $(Pb_3Bi)^{3-}$ and $Bi_4{}^0$. Both options sum up to a total composition of $\{Pb_3Bi_5\}$, which is in accordance with the result of the energy-dispersive X-ray spectroscopy analysis, being $Pb_{3.20}Bi_{4.65}$. To rationalize the former case (a) to be more likely, we first considered the relative atom sizes. Both $(PbBi_3)^-$ and $(Pb_3Bi)^{3-}$ can be viewed as being built up by a triangular base of one atom type, which is then capped by a single atom of the second atom type. As shown in one of our earlier studies, the relative stability of such anions with a 1:3 or 3:1 atomic ratio depend on the respective covalent radii of the involved elements.[21] In the case presented here, however, this should play a minor role only, as the difference of the covalent radii of Pb and Bi is negligible. We thus attribute the preference of (a), $(PbBi_3)^-$ and $(Pb_2Bi_2)^{2-}$, over (b), $(Pb_3Bi)^{3-}$ and $Bi_4{}^0$, to the unfavorable charge distribution in the latter case.

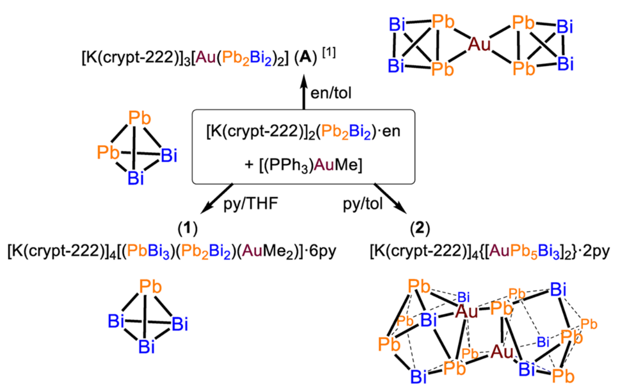

SCHEME 1 Illustration of the formation of compounds **A**,[1] **1** (this work), and **2** (this work) by reactions of $[K(crypt\text{-}222)]_2(Pb_2Bi_2)\cdot en$ with $[AuMePPh_3]$, with the results depending on the chosen mixture of a solvent and a layering agent

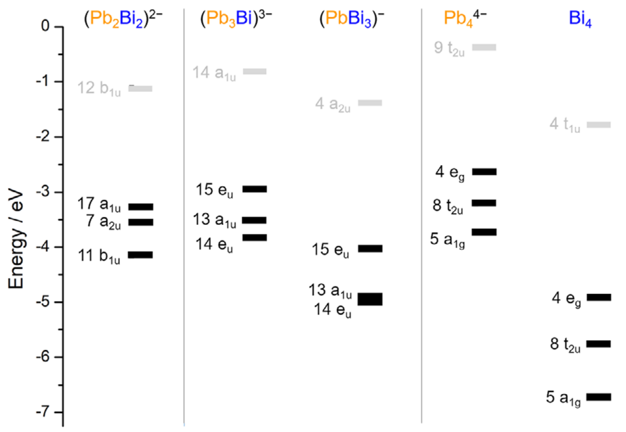

FIGURE 2 Comparison of the energy diagrams of the frontier molecular orbitals of all species indicated in Equation (2): $(Pb_2Bi_2)^{2-}$ (C_{2v} symmetry), $(Pb_3Bi)^{3-}$ (C_{3v} symmetry), $(PbBi_3)^{-}$ (C_{3v} symmetry), $Pb_4{}^{4-}$ (T_d symmetry), and Bi_4 (T_d symmetry). The LUMO level is given in gray shade. All structures were calculated in C_1 symmetry first to avoid bias and then re-optimized in the higher symmetries into which the first optimizations converged. All calculations were done applying COSMO

Remarkably, $(PbBi_3)^{-}$ represents the first (*pseudo*-)tetrahedral anion featuring a single negative charge (−1) that was obtained in condensed phase (Figure 1, left). All other analogous species that were found in crystalline compounds possess different charges, such as $Tl_4{}^{8-}$, $(TlSn_3)^{5-}$, $Pb_4{}^{4-}$, $(Ge_3As)^{3-}$, $(Pb_2Bi_2)^{2-}$, $(TlBi_3)^{2-}$, P_4, and $(P_3S)^{+}$.[1] Thus, the new anion fills a gap in an otherwise seamless series running from charges of +1 to −5. In addition, $(PbBi_3)^{-}$ is the first polyhedral anion, in which tetrel and pnictogen metal atoms occur in a 1:3 ratio. Recently, the reactions of K_3Bi_2 with K_4Sn_9 or $K_{12}Sn_{17}$ in liquid ammonia yielded the planar, $[CO_3]^{2-}$-type $[SnBi_3]^{5-}$ anion.[31] Further $[CO_3]^{2-}$-type $[TtPn_3]^{5-}$ anions exist in several alloy compounds, such as $A_5[TtPn_3]$ (A = Na, K, Rb, Cs; Tt = Si, Ge, Sn; Pn = P, As, Bi).[10] Nevertheless, none of the previously reported that $\{TtPn_3\}$ compounds show a polyhedral structure.

Attempts to crystallize $(PbBi_3)^{-}$ as the only anion have failed so far. We ascribe this to the size of the anion, which is not suited to form a stable crystal together with only one $[K(crypt\text{-}222)]^{+}$ counterion or similar monocationic complexes. The crystals of **1** are insoluble in en, and using $[AuClPPh_3]$ as another source of Au(I) resulted in the precipitation of a yet-unidentified amorphous solid only. Despite that, we assume that $[AuMe_2]^{-}$ formed independently in solution, and it co-crystallized with $(PbBi_3)^{-}$ and $(Pb_2Bi_2)^{2-}$ due to its suitable charge and size. We note in addition that electrospray ionization (ESI) mass spectrometry (MS) carried out on the mother liquor that remains upon isolation of the single crystals of compound **1** (see Figures S11–S15) gives a clear hint toward the concomitant formation of "$(Pb_3Bi)^{3-}$," as the predominant peak can be assigned to the species $\{[K(crypt\text{-}222)](HPb_3Bi)\}^{-}$ (see Figures S11 and S13; note that both in situ-protonation and aggregation with counterions is a typical observation under ESI-MS conditions). Investigation of redissolved single crystals of **1** by means of ESI-MS was impossible owing to the high sensitivity of the compound that led to (visible) decomposition of the solution in the injection syringe before injection into the mass spectrometer.

We additionally performed DFT[32,33] studies for the new $(PbBi_3)^{-}$ anion in **1**, using the program system TURBOMOLE,[34] and employing the TPSS functional[35] and dhf-TZVP basis sets[36,37] with auxiliary

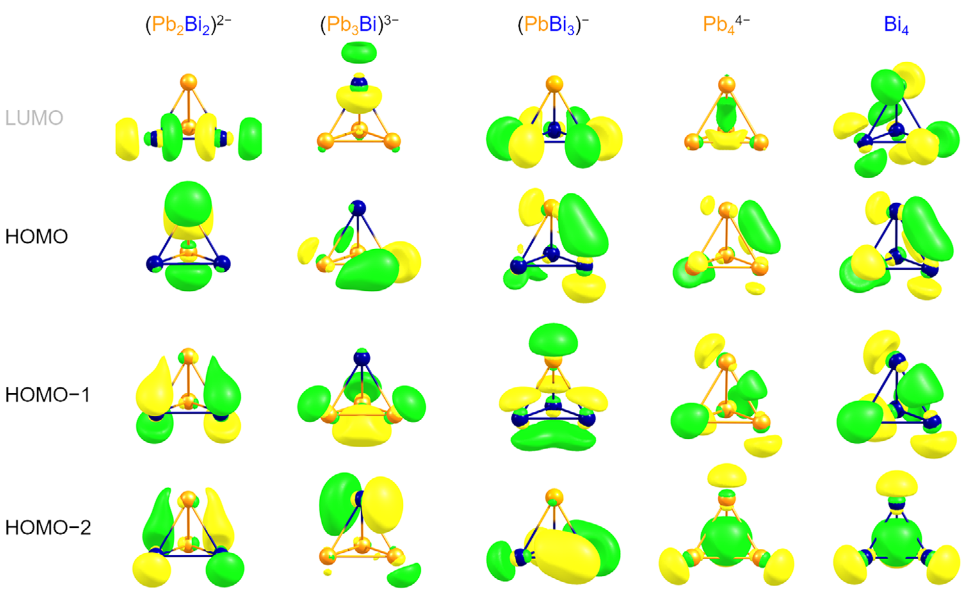

FIGURE 3 Comparison of the contours (plotted at ±0.05 a.u.) of the canonical frontier MOs of all species indicated in Equation (2): $(Pb_2Bi_2)^{2-}$ (C_{2v} symmetry), $(Pb_3Bi)^{3-}$ (C_{3v} symmetry), $(PbBi_3)^{-}$ (C_{3v} symmetry), $Pb_4{}^{4-}$ (T_d symmetry), and Bi_4 (T_d symmetry); Pb atoms: orange, Bi atoms: blue. All structures were calculated in C_1 symmetry first to avoid bias and then re-optimized in the higher symmetries into which the first optimizations converged. In the case of degenerated MOs (see Figure 2), only one is shown as a representative; note that the shown MOs do therefore not host the same total electron counts, but 6 for C_{2v} symmetry, 10 for C_{3v} symmetry, and 12 for T_d symmetry. All calculations were done applying COSMO MOs, molecular orbitals

bases[38] and effective core potentials[39,40] for all atoms. The anion has a reasonably large HOMO–LUMO gap of 2.67 eV, rationalizing the likeliness of its existence. Our calculations showed that the Bi–Bi bonds are 3.00 Å, and thus slightly shorter than the heteroatomic Pb–Bi bonds with 3.05 Å. For the $(Pb_2Bi_2)^{2-}$ anion, the trend is the same: Bi–Bi, Pb–Bi, and Pb–Pb distances are 3.01, 3.06, and 3.08 Å, respectively. Taking into account the typical elongation of bonds in DFT calculations (by 0.01–0.05 Å relative to solid-state structures), the calculated data are in very good agreement with the experimental values (Pb/Bi–Pb/Bi 3.0159(16) and 3.0293(13) Å), which cannot be assigned to the different types of interatomic connections occurring in compounds **1** (Pb–Pb, Pb–Bi, Bi–Bi), though, owing to the nearly identical electron count of both metals, which prevents their differentiation by X-ray diffraction. Natural population analyses[41] showed that the single negative charge is delocalized over all four atoms (Table S7), and localization of the molecular orbitals (MOs) according to *Boys*' method[42] showed only regular two-center bonds (Figure S8). Hence, the calculations confirm that the $(PbBi_3)^-$ anion is reasonably stable, and that the observed structural parameters are in full agreement with those of an anion of the given composition.

To rationalize that this heretofore unprecedented anion actually forms, we compared the MO schemes of the frontier orbitals (Figure 2) and also the contours of the frontier MOs (Figure 3) of all species indicated in Equation (1), which for the elemental combination of Pb and Bi reads in the following equation:

$$2(Pb_2Bi_2)^{2-} \rightleftharpoons (Pb_3Bi)^{3-} + (PbBi_3)^{-}[\rightleftharpoons Pb_4^{4-} + Bi_4]^{\ddagger} \qquad (2)$$

Corresponding reaction energies ΔE_R for the two steps are −48 and +153 kJ mol^{-1}, respectively, confirming that the second step is unlikely to occur under the given reaction conditions.

Notably, the HOMO energy along the series of anions increases with increasing Pb content and decreases with increasing Bi content. The development is not absolutely symmetric though, which also holds for the development of the total energies of the species and is reflected in the clearly exoenergetic formation of the $(Pb_3Bi)^{3-}/(PbBi_3)^-$ pair versus a significantly endoenergetic formation of the $Pb_4{}^{4-}/Bi_4$ pair. Actually, the 1:3 $(PbBi_3)^-$ anion observed in compound **1** seems to be more favorable overall than the inverted 3:1 anion that has not yet been observed in the condensed phase. We attribute this to a much better orbital overlap both of the Bi atoms of the triangular basis (as opposed to a Pb_3 basis) and of Bi and Pb atoms—especially in the HOMO and HOMO-1, see Figure 3. Although not of relevance for the anion in **1**, we note in passing that the comparably high instability of $Pb_4{}^{4-}$ is well visible in the only little overlap of the atomic orbitals in the HOMO ($4e_g$) and HOMO-1 ($8t_{2u}$), which host a total of 10 electrons whereas only the HOMO-2 ($5a_{1g}$) contributed markedly to bonding of the tetrahedron. This is in sharp contrast to the situation in Bi_4, in which all highest occupied MOs indicate significant orbital overlap and thus reasonable bonding interactions. Hence, Bi_4 should be an isolable molecule—and fairly stable as compared to the experimentally observed $(Pb_2Bi_2)^{2-}$ and now $(PbBi_3)^-$. We look forward to seeing this unprecedented Bi modification realized in future work.

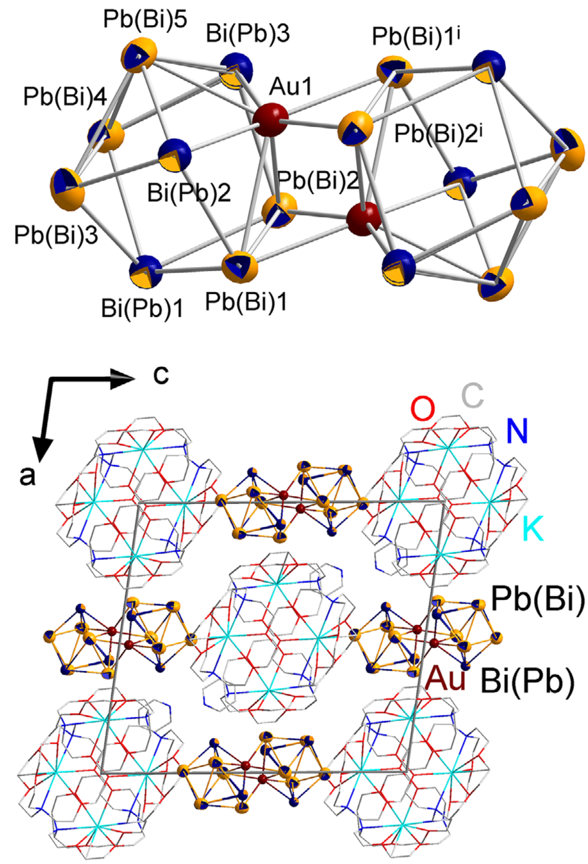

FIGURE 4 Top: Molecular structure of the dimeric cluster anion in **2**. Thermal ellipsoids are drawn at 30% probability. Selected distances [Å] and angles [°]: Pb1–Pb2 3.310(2), Pb3–Pb4 3.132(2), Pb(3,4)–Pb5 3.191(2)–3.1922(19), Bi1–Pb 3.071(2)–3.126(2), Bi(2,3)–Pb 3.016(6)–3.098(6), Au1–Pb(1^i,2^i) 2.8671(7)–2.8951(12), Au1···Pb(1,2) 3.167(2)–3.2067(18), Au1···Pb5 3.098(6), Au–Bi 2.835(2)–2.867(5), Au···Au 2.869(3); Pb1···Au1···Pb2 62.57(5), Pb1^i–Au1–Pb2^i 69.97(6), Pb(1^i,2^i)–Au···Pb(2,1) 87.57(6), 88.08(5), Pb(1^i,2^i)–Au···Pb(1,2) 123.58(5), 124.17(5), Bi–Au–Bi 120.33(14), Bi(2,3)–Au–Pb(2^i,1^i) 84.35(6), 83.60(14), Bi(2,3)–Au–Pb(1^i,2^i) 153.01(6), 152.64(15), Pb(1,2) ···Au–Bi(2,3) 61.40(5), 59.23(11), Pb(1,2)···Au–Bi(3,2) 113.25(13), 114.60(7). Symmetry code: i = −*x*, −*y*, 1 − *z*. For more details, see Figures S1, S3, S7, and Tables S1, S3, S6. Bottom: View of the (extended) unit cell of **2** along the crystallographic *b* axis. [K(crypt-222)]$^+$ cations are shown in wire mode for clarity

We anticipated that the fragmentation/reorganization process would get even more complex, as the crystalline yield of **1** allowed for more compounds to form. We therefore altered the crystallization conditions by changing the solvent for layering from THF to toluene, whereas all other reaction conditions were kept the same. The observation of a different product to crystallize indicated the high tendency for the $(Pb_2Bi_2)^{2-}$ anion to undergo more significant reconstruction processes, which in turn renders the observation of the new anion in **1** a lucky circumstance.

Compound **2** crystallizes as black needles in the monoclinic crystal system, space group type $P2_1/n$ (approx. 40% yield). It is based on the ternary cluster anion $\{[AuPb_5Bi_3]_2\}^{4-}$ (Figure 4). $\{[AuPb_5Bi_3]_2\}^{4-}$ represents the yet-missing heaviest homolog of an isostructural series of

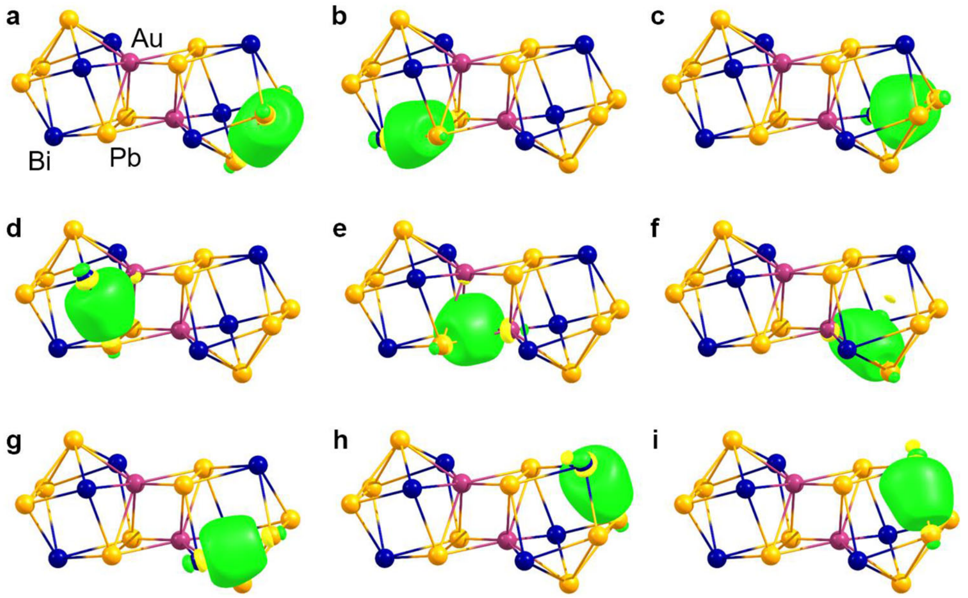

FIGURE 5 Representative LMOs for the bonds in anion **2**: Three-center bonds (a–c), three-center bonds involving the Au atoms (d–f), regular two-center bonds (g and h), polarized two-center bond (i). Contour values are drawn at ±0.05 a.u. LMO, localized molecular orbitals

such dimers of trimetallic 9-vertex cages, $\{[AuTt_5Pn_3]_2\}^{4-}$ (Tt = Sn, Pb; Pn = Sb, Bi) and $\{[CuSn_5Sb_3]_2\}^{4-}$.[20,43] The assignment of the Pb and Bi atoms was done by means of quantum chemical calculations again. According to these results, we find the preferred distribution of the Pb and Bi atoms to be analogous to that in the lighter homologs. Figure 4 illustrates the assignment by the chosen predominant color of the two-colored thermal ellipsoids. The calculated bond lengths and angles also follow the expected trends and accord with the experimentally observed ones.

As for the lighter homologs of this series we do not find any Au···Au interactions. The Au atoms form instead three-center bonds with most of the surrounding Pb and Bi atoms, namely Au1–Bi2–Pb5, Au1–Bi3–Pb5, Au1–Pb1–Bi2, as well as Au1–Pb1^{i}–Pb2^{i}. Additionally we find two- or three-center bonds between the other Pb and Bi atoms, which are slightly polarized (see Figure 5).

As already shown in Scheme 1, the syntheses of **1**, **2**, and **A** greatly depend on the solvents used during the reaction and the layering step. In contrast, the products that are reproducibly obtained from these reactions are independent from the ratio of the reactants, as the three compounds were isolated as the only crystal types from the corresponding Schlenk tubes (with the reactant ratios ranging from 1:3 to 3:1), respectively. This is in contrast to the recently reported Au/Sn/Sb systems, where not only the solvent, but also the reactant ratios significantly influenced the composition of the isolated compounds.[27]

For further comparison, we additionally investigated the Au/Pb/Sb system and performed the reactions between $[K(crypt\text{-}222)]_2(Pb_2Sb_2)\cdot en$ and $[AuMePPh_3]$, from which $[K(crypt\text{-}222)]_4\{[AuPb_5Sb_3]_2\}\cdot 3en$ (**B·3en**) was previously isolated from en/tol.[20] The same reaction carried out in either py/tol or py/THF resulted in the crystallization of the same compound, yet with different co-crystallizing solvent molecules, **B·2py** (see Figures S1, S4, S6 and Tables S1, S4, S5). Although the underlying formation mechanism could not yet be unraveled, as typical for inorganic cluster syntheses, we may conclude that the results observed in this series of reactions are strongly dependent on the ratios of the atomic radii of the involved elements and thus explain the differences found for the Au/Pb/Bi versus Au/Sn/Sb versus Au/Pb/Sb combination.

CONCLUSIONS

In summary, we reported the formation of the salts of two new anions $(PbBi_3)^-$ and $\{[AuPb_5Bi_3]_2\}^{4-}$, which were synthesized under the same reaction conditions while crystallized from different solvent combinations. The $(PbBi_3)^-$ in **1** represents the first experimental proof for the existence of a (*pseudo*-)tetrahedral molecule with a single charge in condensed phase, which closes a gap in a series of related molecules with charges running from +1 to −5. At the same time, the $(PbBi_3)^-$ anion is the first *pseudo*-tetrahedral unit comprising tetrel and pnictogen atoms in a 1:3 ratio, which finally rationalizes the exchange process for 2:2 anions in solution to occur. The $\{[AuPb_5Bi_3]_2\}^{4-}$ cluster anion in **2** represents the heaviest homolog in the $\{[MTt_5Pn_3]_2\}^{4-}$ series and illustrates the distinct tendency of the initial species $(Pb_2Bi_2)^{2-}$ to undergo more complex fragmentation/rearrangement processes in solution.

Together with the anion in **1** and the recently reported compound $[Au\{\eta^2\text{-}(Pb_2Bi_2)\}_2]^{3-}$, the anion in **2** demonstrates the importance of the chosen crystallization conditions for the product spectrum in terms of maintaining an intact geometry, performing atom exchange, or more significant fragmentation and reconstruction. Future studies will be focused on the in-depth studies of the roles of solvents in the cluster formation mechanisms and prediction of selective and efficient formation pathways. In addition, we will explore the reactivities of **1** toward a variety of d-/f-/p-block metal precursors.

ACKNOWLEDGMENTS

This work was financially supported by the German Research Foundation (Deutsche Forschungsgemeinschaft, DFG). F.P. gratefully acknowledges a research fellowship by the Alexander von Humboldt foundation.

CONFLICT OF INTEREST

Stefanie Dehnen is a coauthor of the manuscript and a member of the Advisory Board of Natural Sciences and was not involved at the handling of the peer-review process of this submission. All other authors have no conflict of interest.

ETHICS STATEMENT

There are no ethical issues to consider in this work.

AUTHOR CONTRIBUTIONS

The manuscript was written through contributions of all authors. All authors have given approval to the final version of the manuscript.

DATA AVAILABILITY STATEMENT

All data generated or analyzed during this study are included in this published article and its Supporting Information.

The structures of compounds **1**, **2**, and **B·2py** were determined by single-crystal X-ray diffraction. The crystallographic data for the two structures reported in this paper have been deposited with the Cambridge Crystallographic Data Centre as supplementary publications nos. CCDC-2142405 (**1**), CCDC-2142406 (**2**), and CCDC-2142405 (**B·2py**). Copies of the data can be obtained free of charge on application to CCDC, 12 Union Road, Cambridge CB2 1EZ, UK [fax.: (internat.) + 44 1223/336-033; e-mail: deposit@ccdc.cam.ac.uk]. Further details are provided in the Supplementary Information.

The Cartesian coordinates of all optimized structures and the respective SCF energies are summarized in the supplementary document “optimized-structures.txt.” The files comprise all necessary data for reproducing the values. Information on the used methods and corresponding references are provided in the Supporting Information. For the default parameters of TURBOMOLE, such as the convergence criteria for structure optimizations, please see the manual at https://www.turbomole.org (retrieved April 23, 2022).

PEER REVIEW

The peer review history for this article is available at https://publons.com/publon/10.1002/ntls.202103302

ORCID

Fuxing Pan https://orcid.org/0000-0002-3798-4213
Lukas Guggolz https://orcid.org/0000-0002-0415-8089
Stefanie Dehnen https://orcid.org/0000-0002-1325-9228

REFERENCES

1. Pan F, Guggolz L, Dehnen S. Cluster chemistry with (*pseudo*-)tetrahedra involving group 13–15 (semi-)metal atoms. *CCS Chem*. 2021;3:2969–2984.
2. Riu M-LY, Jones RL, Transue WJ, Müller P, Cummins CC. Isolation of an elusive phosphatetrahedrane. *Sci Adv*. 2020;6(13):eaaz3168.
3. Hierlmeier G, Coburger P, Bodensteiner M, Wolf R. Di-*tert*-butyldiphosphatetrahedrane: catalytic synthesis of the elusive phosphaalkyne dimer. *Angew Chem Int Ed*. 2019;58(47):16918–16922.
4. Riu M-LY, Ye M, Cummins CC. Alleviating strain in organic molecules by incorporation of phosphorus: synthesis of triphosphatetrahedrane. *J Am Chem Soc*. 2021;143(40):16354–16357.
5. Jupp AR, Slootweg JC. Mixed phosphatetrahedranes. *Angew Chem Int Ed*. 2020;59(27):10698–10700.
6. Cossairt BM, Diawara M-C, Cummins CC. Facile synthesis of AsP_3. *Science*. 2009;323(5914):602.
7. Cossairt BM, Cummins CC. Properties and reactivity patterns of AsP_3: an experimental and computational study of group 15 elemental molecules. *J Am Chem Soc*. 2009;131(42):15501–15511.
8. Weis P, Röhner DC, Prediger R, et al. First experimental evidence for the elusive tetrahedral cations $[EP_3]^+$ (E = S, Se, Te) in the condensed phase. *Chem Sci*. 2019;10(46):10779–10788.
9. Wilson RJ, Lichtenberger N, Weinert B, Dehnen S. Intermetalloid and heterometallic clusters combining p-block (semi) metals with d-or f-block metals. *Chem Rev*. 2019;119(14):8506–8554.
10. Pan F, Weinert B, Dehnen S. Binary Zintl anions involving group 13–15 (semi-)metal atoms, and the relationship of their structures to electron count. *Struct Bond*. 2021;188:103–148.
11. Peters B, Lichtenberger N, Dornsiepen E, Dehnen S. Current advances in tin cluster chemistry. *Chem Sci*. 2020;11(1):16–26.
12. Weinert B, Dehnen S. Binary and ternary intermetalloid clusters. *Struct Bond*. 2017;174:99–134.
13. Waibel M, Kraus F, Scharfe S, Wahl B, Fässler TF. $[(MesCu)_2(\eta^3\text{-}Si_4)]^{4-}$: a mesitylcopper-stabilized tetrasilicide tetraanion. *Angew Chem Int Ed*. 2010;49(37):6611–6615.
14. Stegmaier S, Waibel M, Henze A, Jantke LA, Karttunen AJ, Fässler TF. Soluble Zintl phases $A_{14}ZnGe_{16}$ (A = K, Rb) featuring $[(\eta^3\text{-}Ge_4)Zn(\eta^2\text{-}Ge_4)]^{6-}$ and $[Ge_4]^{4-}$ clusters and the isolation of $[(MesCu)_2(\eta^3{:}\eta^3\text{-}Ge_4)]^{4-}$: the missing link in the solution chemistry of tetrahedral group 14 element Zintl clusters. *J Am Chem Soc*. 2012;134(35):14450–14460.
15. Wallach C, Mayer K, Henneberger T, Klein W, Fässler TF. Intermediates and products of the reaction of Zn(ii) organyls with tetrel element Zintl ions: cluster extension versus complexation. *Dalton Trans*. 2020;49(19):6191–6198.
16. Fendt F, Koch C, Gärtnera S, Korber N. Reaction of Sn_4^{4-} in liquid ammonia: the formation of $Rb_6[(\eta^2\text{-}Sn_4)Zn(\eta^3\text{-}Sn_4)]\cdot 5NH_3$. *Dalton Trans*. 2013;42(44):15548–15550.
17. Klem MT, Corbett JD. A_5InPb_8 (A = K, Rb): an apparent Zintl phase with lead tetrahedra interbridged by μ^6-In atoms. *Inorg Chem*. 2005;44(17):5990–5995.
18. Mitzinger S, Broeckaert L, Massa W, Weigend F, Dehnen S. Understanding of multimetallic cluster growth. *Nat Commun*. 2016;7:10480–10490.
19. Mitzinger S, Bandemehr J, Reiter K, et al. $(Ge_2P_2)^{2-}$: a binary analogue of P_4 as a precursor to the ternary cluster anion $[Cd_3(Ge_3P)_3]^{3-}$. *Chem Commun*. 2018;54(12):1421–1424.
20. Pan F, Guggolz L, Weigend F, Dehnen S. Atom exchange versus reconstruction: $(Ge_xAs_{4-x})^{x-}$ (x = 2, 3) as building blocks for the supertetrahedral Zintl cluster $[Au_6(Ge_3As)(Ge_2As_2)_3]^{3-}$. *Angew Chem Int Ed*. 2020;59(38):16638–16643.
21. Guggolz L, Dehnen S. Systematic DFT studies on binary pseudo-tetrahedral Zintl anions: relative stabilities and reactivities towards

protons, trimethylsilyl groups, and iron complex fragments. *Chem Eur J*. 2020;26(51):11819–11828.
22. Lichtenberger N, Wilson RJ, Eulenstein AR, et al. Main group metal-actinide magnetic coupling and structural response upon U^{4+} inclusion into Bi, Tl/Bi, or Pb/Bi cages. *J Am Chem Soc*. 2016;138(29):9033–9036.
23. Eulenstein AR, Franzke YJ, Lichtenberger NR, et al. Substantial π-aromaticity in the anionic heavy-metal cluster $[Th@Bi_{12}]^{4-}$. *Nat Chem*. 2021;13:149–155.
24. Pan F, Wei S, Guggolz L, Eulenstein A, Tambornino F, Dehnen S. Insights into formation and relationship of multimetallic clusters – on the way towards Bi-rich nanostructures. *J Am Chem Soc*. 2021;143(18):7176–7188.
25. Lichtenberger N, Massa W, Dehnen S. Polybismuthide anions as ligands: the homoleptic complex $[(Bi_7)Cd(Bi_7)]^{4-}$ and the ternary cluster $[(Bi_6)Zn_3(TlBi_5)]^{4-}$. *Angew Chem Int Ed*. 2019;58(10):3222–3226.
26. Pan F-X, Li L-J, Sun Z-M. $[Au(\eta^2\text{-}Sn_2Sb_2)_2]^{3-}$: a mixed group 14/15 tetrahedral dimer bridged by Au. *Chin J Struct Chem*. 2016;35:1099–1106.
27. Pan F, Lukanowski M, Weigend F, Dehnen S. Tetrahedral $[Sb(AuMe)_4]^{3-}$ occurring in multimetallic cluster syntheses: about the structure-directing role of methyl groups. *Angew Chem Int Ed*. 2021;60(47):25042–25047.
28. Zhu D, Lindeman SV, Kochi JK. X-ray crystal structures and the facile oxidative (Au–C) cleavage of the dimethylaurate(I) and tetramethylaurate(III) homologues. *Organometallics*. 1999;18(11):2241–2248.
29. Klemm W. Metalloids and their compounds with the alkali metals. *Proc Chem Soc*. 1958;329–364.
30. Busmann E. Das Verhalten der Alkalimetalle zu Halbmetallen. X. Die Kristallstrukturen von KSi, RbSi, CsSi, KGe, RbGe und CsGe. *Z Anorg Allg Chem*. 1961;313(1–2):90–106.
31. Mayer K, Dums JV, Klein W, Fässler TF. $[SnBi_3]^{5-}$ – a carbonate analogue comprising exclusively metal atoms. *Angew Chem Int Ed*. 2017;56(47):15159–15163.
32. Eichkorn K, Treutler O, Öhm H, Häser M, Ahlrichs R. Auxiliary basis sets to approximate Coulomb potentials. *Chem Phys Lett*. 1995;240(4):283–290.
33. Eichkorn K, Weigend F, Treutler O, Ahlrichs R. Auxiliary basis sets for main row atoms and transition metals and their use to approximate Coulomb potentials. *Theor Chem Acc*. 1997;97:119–124.
34. TURBOMOLE V7.5 2020, a development of University of Karlsruhe and Forschungszentrum Karlsruhe GmbH, 1989–2007, TURBOMOLE GmbH, since 2007; available from http://www.turbomole.com
35. Tao J, Perdew JP, Staroverov VN, Scuseria GE. Climbing the density functional ladder: nonempirical meta–generalized gradient approximation designed for molecules and solids. *Phys Rev Lett*. 2003;91(14):3–6.
36. Weigend F, Ahlrichs R. Balanced basis sets of split valence, triple zeta valence and quadruple zeta valence quality for H to Rn: design and assessment of accuracy. *Phys Chem Chem Phys*. 2005;7(18):3297–3305.
37. Weigend F, Baldes A. Segmented contracted basis sets for one- and two-component Dirac–Fock effective core potentials. *J Chem Phys*. 2010;133(17):174102.
38. Weigend F. Accurate Coulomb-fitting basis sets for H to Rn. *Phys Chem Chem Phys*. 2006;8(9):1057–1065.
39. Metz B, Stoll H, Dolg M. Small-core multiconfiguration-Dirac–Hartree–Fock-adjusted pseudopotentials for post-d main group elements: application to PbH and PbO. *J Chem Phys*. 2000;113(7):2563.
40. Figgen D, Rauhut G, Dolg M, Stoll H. Energy-consistent pseudopotentials for group 11 and 12 atoms: adjustment to multi-configuration Dirac–Hartree–Fock data. *Chem Phys*. 2005;311(1–2):227–244.
41. Reed AE, Weinstock RB, Weinhold F. Natural population analysis. *J Chem Phys*. 1985;83(2):735–746.
42. Boys SF. In: Löwdin P-O, ed. *Quantum Theory of Atoms, Molecules and the Solid State*. 1st ed. Academic Press; 1966:253–262.
43. Wilson RJ, Broeckaert L, Spitzer F, Weigend F, Dehnen S. $\{[CuSn_5Sb_3]^{2-}\}_2$: a dimer of inhomogeneous superatoms. *Angew Chem Int Ed*. 2016;55(39):11775–11780.

SUPPORTING INFORMATION

Additional supporting information can be found online in the Supporting Information section at the end of this article.

How to cite this article: Pan F, Guggolz L, Dehnen S. Capture the missing: formation of $(PbBi_3)^-$ and $\{[AuPb_5Bi_3]_2\}^{4-}$ via atom exchange or reorganization of the *pseudo*-tetrahedral Zintl anion $(Pb_2Bi_2)^{2-}$. *Nat Sci*. 2022;2:e202103302. https://doi.org/10.1002/ntls.202103302